A prototype of a highly sensitive cryogenic current comparator with a HTS SQUID and HTS magnetic shield

2004 Supercond. Sci. Technol. 17 S450

(http://iopscience.iop.org/0953-2048/17/5/073)

INSTITUTE OF PHYSICS PUBLISHING SUPERCONDUCTOR SCIENCE AND TECHNOLOGY

Supercond. Sci. Technol. **17** (2004) S450–S455 PII: S0953-2048(04)76979-1

A prototype of a highly sensitive cryogenic current comparator with a HTS SQUID and HTS magnetic shield

T Watanabe[1,5], S Watanabe[2], T Ikeda[1], M Kase[1], Y Sasaki[3], T Kawaguchi[4] and T Katayama[1,2]

[1] RIKEN (The Institute of Physical and Chemical Research), 2-1 Hirosawa, Wako-shi, Saitama 351-0198, Japan
[2] Center for Nuclear Study, Graduate School of Science, University of Tokyo (CNS), 2-1 Hirosawa, Wako-shi, Saitama 351-0198, Japan
[3] Matsushita Electric Industrial, 3-1-1 Yagumonakamachi, Moriguchi, Osaka 570-8501, Japan
[4] KT Science Ltd, 1470-1-803 Fujie, Akashi-shi, Hyogo 673-0162, Japan

E-mail: wtamaki@postman.riken.go.jp (T Watanabe)

Received 1 March 2004
Published 20 April 2004
Online at stacks.iop.org/SUST/17/S450
DOI: 10.1088/0953-2048/17/5/073

Abstract

A highly sensitive cryogenic current comparator (CCC) for the measurement of the intensity of faint beams, such as a radioisotope beam, was developed for the RIKEN RI beam factory project. This monitor is composed of a high-temperature superconducting (HTS) magnetic shield and an HTS current sensor including an HTS superconducting quantum interference device (SQUID), which are cooled by a low-vibration pulse-tube refrigerator. Both the HTS magnetic shield and the HTS current sensor based on Bi_2–Sr_2–Ca_2–Cu_3–O_x (Bi-2223) were fabricated by dip-coating on a 99.9% MgO ceramic substrate. Recently, a prototype of the HTS SQUID CCC system was completed and we carried out the first measurements using DC ion beams in the current range of 0.5–20 μA, which were produced by the ECR (electron cyclotron resonance) ion source in the CNS experimental hall. After the measurement was successfully carried out in the CNS, we installed the system into the beam transport line of the RIKEN Ring Cyclotron (RRC) to measure the current of the high-energy heavy-ion beam which has a bunched microstructure. In this paper, we describe the performance and the present status of the prototype of the HTS SQUID CCC system and the results of the ion beam measurement.

(Some figures in this article are in colour only in the electronic version)

1. Introduction

Beam diagnostics are essential constituents of any accelerator, and total current is one of the most important parameters for operating an accelerator efficiently and for improving the performance of the machine. A DC current transformer (DCCT) based on the second-harmonic modulator–demodulator has been used in circular accelerators, the sensitivity of which is approximately 1 μA [1]. On the other hand, a new type of CCC using a low-temperature superconducting (LTS) magnetic shield and an LTS SQUID was developed to measure ion beams extracted from SIS, the heavy-ion synchrotron at GSI in Germany [2]. The intensities of the faint ion beams are below the lowest measurable limit of the DCCT. In addition, an LTS CCC for measuring a low beam current of nanoampere to microampere order was constructed for atomic-physics experiments at the heavy-ion cooler synchrotron TARN II [3].

[5] Author to whom any correspondence should be addressed.

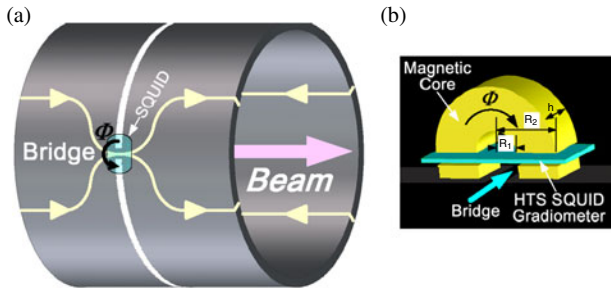

Figure 1. (a) A schematic drawing of the current sensor of the HTS CCC. (b) Structure consisting of the SQUID gradiometer and the magnetic core near the bridge.

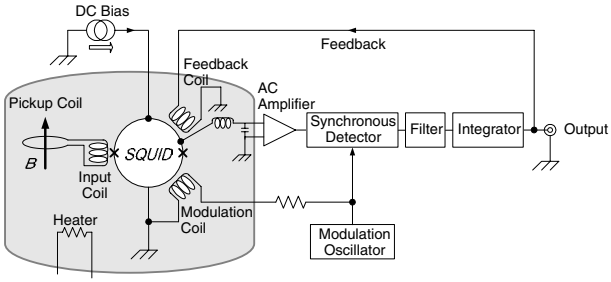

Figure 2. Circuit diagram of the HTS DC SQUID (2 Josephson junctions) and flux-locked loop. The sensor package (hatched region) in the box is kept below the critical temperature T_c.

An accurate and nondestructive current measurement is essential for determining the reaction cross section in cooler-ring experiments. Furthermore, Hao *et al* [4] reported that a prototype HTS CCC with an HTS gradiometer SQUID was successfully demonstrated as a means of nondestructive sensing of argon beams in the current range of 1–20 μA. The HTS technology enables us to develop a system equipped with a downsized and highly sensitive current monitor with an HTC SQUID and an HTS magnetic shield. Thus, the highly sensitive HTS SQUID CCC for the measurement of the intensity of faint beams, such as a radioisotope beam, was developed for the RIKEN RI beam factory project [5–8].

2. The principle of the HTS SQUID CCC

The principle of the superconductive CCC is based on the Meissner effect of superconducting materials. A schematic drawing of the current sensor of the HTS CCC is shown in figure 1(a). The MgO ceramic tube used as the substrate of the HTS magnetic shield is coated on both sides, inside and outside, with a thin layer (300 μm) of HTS material. When a charged particle (ion or electron) beam is being passed along the axis of the HTS tube, a shielding current produced by the Meissner effect flows in the opposite direction along the wall of the HTS tube so as to screen the magnetic field generated by the beam. Since the outer surface is designed to have a bridge circuit (see figure 1(a)), the current generated by the charged particle beam concentrates in the bridge circuit and forms an azimuthal magnetic field Φ around it. Moreover, the HTS SQUID is close to the bridge circuit and can detect the azimuthal magnetic field with a high S/N ratio. In particular, since the SQUID gradiometer has two pickup coils that are wound in opposite directions and connected in series, the signal level is expected to be improved by a factor of 2, while the background noise can then be significantly reduced by more than 40 dB. Furthermore, to obtain a higher coupling efficiency, we are investigating the possibility of introducing a high-permeability magnetic core in the HTS CCC. The sketch (figure 1(b)) represents a structure consisting of the SQUID gradiometer and the magnetic core near the bridge.

3. Equipment

3.1. HTS SQUID system

The HTS DC SQUID system, which is composed of an HTS SQUID gradiometer (Y–Ba_2–$Cu_3O_{7-\delta}$) [9], a cryogenic cable,

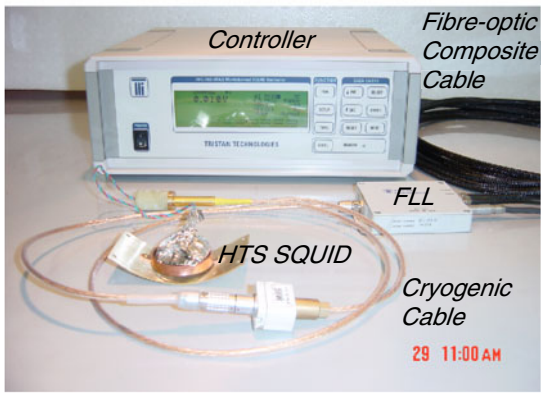

Figure 3. The HTS DC SQUID system Model BMS-G with HTG-10R (see footnote 6).

a flux-locked loop module, a fibre-optic composite cable that connects the flux-locked loop module to control electronics, and a set of control electronics, is commercially available[6]. Figure 2 shows the circuit diagram of the HTS DC SQUID (2 Josephson junctions) and flux-locked loop. The sensor package (hatched region) in the box is kept below the critical temperature T_c. The magnetic flux density B induced by the charged particle beam is transferred to the HTS SQUID with the aid of the pickup coil and the input coil, which are built into the HTS SQUID itself. The flux-locked loop enables a linear operation with respect to the HTS SQUID circuit because it cancels the external magnetic flux density B by using the feedback coil, as shown in figure 2. This circuit is composed of a DC bias source, a modulation oscillator and a synchronous detector which are used to create a flux-locked loop circuit, a filter and an integrator. A heater is mounted close to the SQUID in the sensor package in order to purge any magnetic flux trapped in the sensor. The fibre-optic composite cable is used to eliminate grounding and shielding problems that often affect SQUID electronics. The HTS DC SQUID system model BMS-G with HTG-10R is shown in figure 3 and the specifications of the system are given in table 1. The HTS SQUID gradiometer is composed of an input coil and SQUID loop which has two Josephson junctions (see figure 4(a)). Figure 4(b) shows the measured noise spectrum in the frequency domain, and indicates a $1/f$ noise structure. White noise is quite low compared with the case of using a conventional HTS SQUID in

[6] Model BMS-G with HTG-10R manufactured by TRISTAN TECHNOLOGIES.

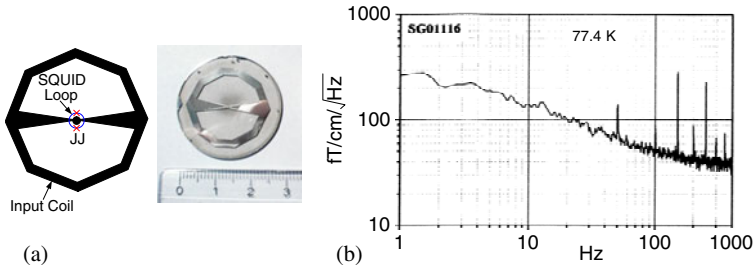

Figure 4. (a) A schematic drawing and picture of the HTS SQUID gradiometer. (b) The measured noise spectrum in the frequency domain, showing a $1/f$ noise structure. White noise is quite low compared with the case of using a conventional HTS SQUID in which white noise is over 1 pT cm^{-1} Hz$^{-1/2}$.

Table 1. Specifications of the HTS DC SQUID system.

Noise level	34 fT cm^{-1} Hz$^{-1/2}$ @ 5 kHz
Operation temperature	77 K
Feedback gain	1, 2, 5, 10, 20, 50, 100, 200, 500
High-pass filter	DC, 0.3 Hz
Low-pass filter	5 Hz, 500 Hz, 5 kHz, 25 kHz
Data accuracy (AD)	16 bit
Data acquisition rates	20 000 words s^{-1}
Remote control	IEEE-488, RS-232

which white noise is over 1 pT cm^{-1} Hz$^{-1/2}$. The coefficient of the magnetic field and the output voltage of the SQUID gradiometer is 2.43 nT V^{-1} when the maximum gain of 500 is selected.

3.2. HTS and permalloy shields

A cylindrical Bi_2–Sr_2–Ca_2–Cu_3–O_x (Bi-2223) HTS magnetic shield (148 mm diameter and 250 mm length) was fabricated by dip-coating (300 μm) on a 99.9% MgO ceramic substrate. An HTS magnetic shield has an advantage in that the magnetic shielding effect is independent of the frequency of environmental magnetic noise, even in the low-frequency band [10]. The critical current (I_c) of 4500 A cm^{-2} and the critical temperature (T_c) of 106 K of the Bi-2223 cylindrical HTS shield were obtained by a DC four-probe method using a small sample of Bi-2223. In order to measure the field distribution inside the HTS shield and to obtain the attenuation factors, we constructed a measurement system [11]. The system is composed of an X–Y–Z stage driven by stepping motors, a G10-rod which is fixed on the X–Y–Z stage and attached to two HTS-SQUID probes, a LN_2 Dewar vessel and a Helmholtz coil that supplies an external field. Hereafter, we define the direction of the cylindrical axis as the z-direction and the direction perpendicular to the axis as the r-direction. If the external fields B_{z0} and B_{r0} exist, the attenuation factors $S_z(z)$ and $S_r(z)$ are defined as

$$S_z(z) = B_z(z)/B_{z0},$$

$$S_r(z) = B_r(z)/B_{r0},$$

where $B_z(z)$ and $B_r(z)$ are the z- and r-components of the magnetic field at position z, respectively. Figure 5 shows the measurement results for attenuation factors $S_z(z)$ and $S_r(z)$, where the directions of the external magnetic field B_0 (3.5 μT, 1 Hz) are the z-direction (•) and x-direction (○), respectively.

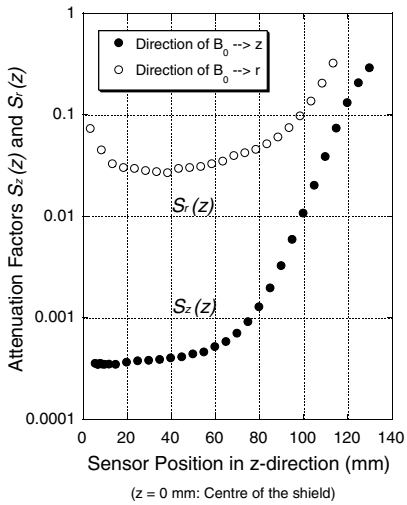

Figure 5. Measurement results for attenuation factors $S_z(z)$ and $S_r(z)$, where the directions of the external magnetic field B_0 (3.5 μT, 1 Hz) are the z-direction (•) and x-direction (○), respectively.

From these measurement results, the attenuation factors of $S_z(0) = 5 \times 10^{-4}$ and $S_r(0) = 8 \times 10^{-2}$ were obtained. Because the attenuation factor of $S_r(0)$ of the HTS magnetic shield is inadequate, we undertook to reinforce the HTS magnetic shield. On the basis of various calculations using the finite element method program OPERA-3d [Note 7] three parts of permalloy shields, permalloy 1, permalloy 2 (disc) and permalloy 2 (cylinder), were constructed around the HTS shield, as shown in figure 6(a). One of the calculations showed that the shielding effect with a chimney-like cylinder shield (see figure 6(a)) is three times higher than that without the shield. In order to confirm the shielding effect of the reinforced system, a measurement was carried out. A field of 10^{-5} T produced by a Helmholtz coil was attenuated to 10^{-11} T, which was measured by the SQUID. A strong magnetic shielding system having an attenuation factor of 10^{-6} was obtained.

3.3. The HTS SQUID CCC system

A schematic drawing of the HTS SQUID CCC system is shown in figure 6(b). The HTS magnetic shield and the HTS current sensor including the HTS SQUID are cooled by a low-vibration pulse-tube refrigerator which has a refrigeration power of 11 W at a temperature of 77 K. The operation temperature can be set

[7] Vector Fields Inc., UK.

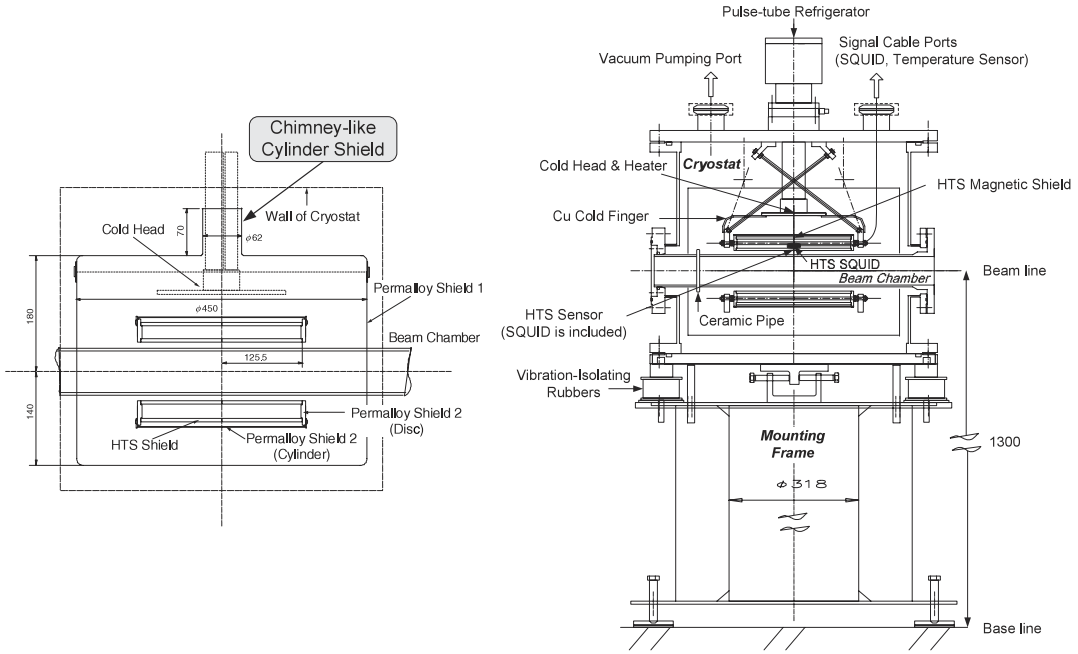

Figure 6. (a) Magnetic shields are composed of an HTS shield, permalloy 1, permalloy 2 (disc) and permalloy 2 (cylinder). (b) A schematic drawing of the SQUID current monitor system.

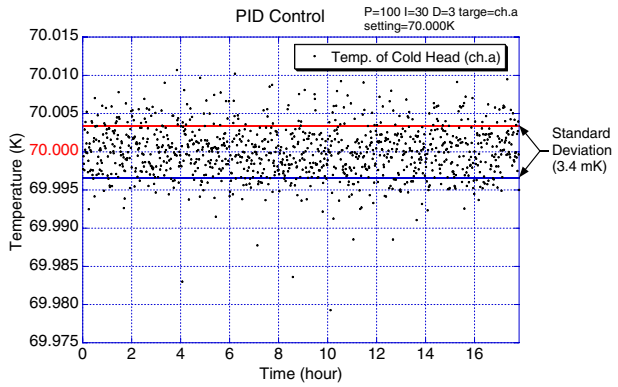

Figure 7. Plots of the temperature of the cold head as a function of time. The standard deviation of the temperature over a period of 18 h was 3.4 mK.

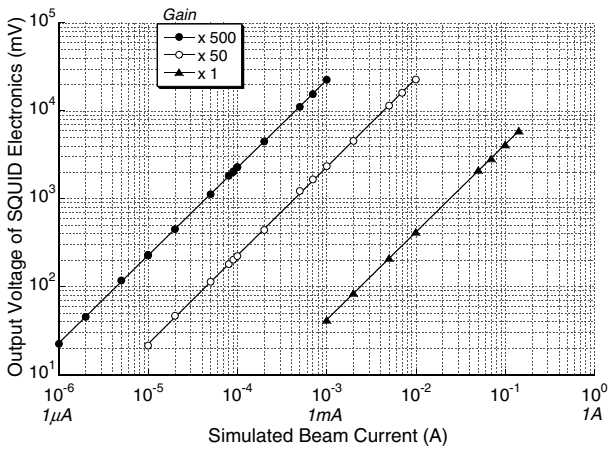

Figure 8. The plotted output voltage of the SQUID electronics as a function of the simulated beam current.

between 64 and 90 K (the critical temperature of the HTS SQUID) using a heater, since the pulse-tube refrigerator is capable of cooling the system to a temperature lower than liquid-nitrogen temperature. Furthermore, it is possible to stabilize the temperature of the HTS SQUID with an accuracy of 5 mK using a PID feedback controller which has four thermometers and a heater. Figure 7 shows plots of the temperature of the cold head as a function of time. The standard deviation of the temperature over a period of 18 h was 3.4 mK.

4. Results of the ion beam test of the HTS SQUID CCC

Prior to the ion beam test, we carried out an off-line test. In order to investigate noise sources, not only the vibration originating from the ground but also that generated by the pulse-tube refrigerator itself were analysed using accelerometers and an FFT in time and frequency domains. We calculated the eigenfrequency of the HTS SQUID CCC and selected eight vibration-isolating rubbers (see figure 6(a)) which can damp the vibration excited by the pulse-tube refrigerator, whose pumping frequency is 5.5 Hz, and there was no problem due to vibration. As a result, the amplitude of the vibration was found to be within 6 μm. Next, the first output signal was observed by feeding a 1 μA sine wave (3 Hz) into a Cu rod which was set in the beam chamber. We confirmed that the measured beam current is not dependent on the beam position or beam radius by changing the position and the radius of the Cu rod. Furthermore, the output voltage of the SQUID electronics as a function of the simulated beam current is plotted in figure 8. The dynamic range of 100 dB (from 1 μA to 0.1 A) was obtained by changing the feedback gain of the SQUID electronics. Recently, we carried out the first beam

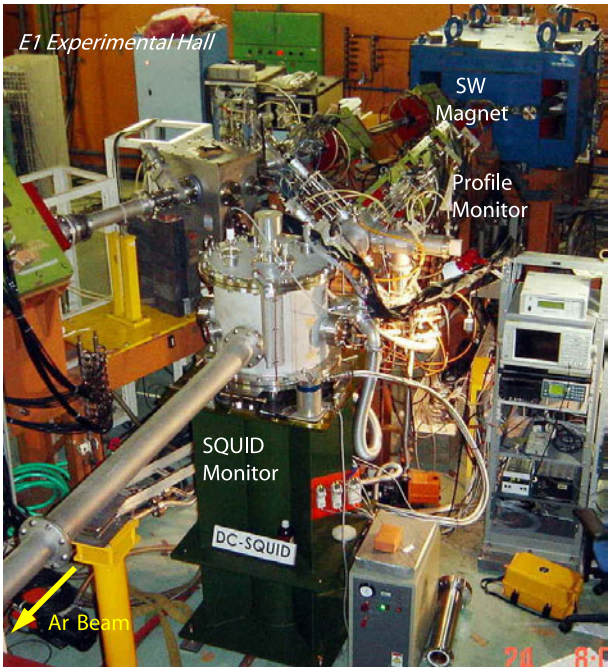

Figure 9. The beam transport line (E1 experimental hall) of the RIKEN Ring Cyclotron (RRC).

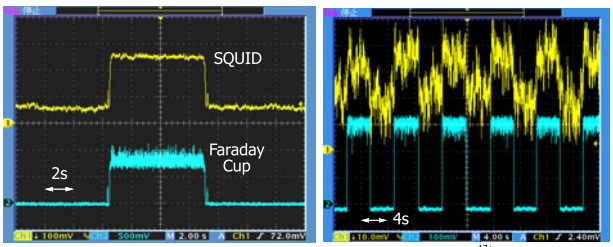

Figure 10. Measured signals of the HTS SQUID CCC (above) and those of the Faraday cup monitor (below) where a 7 μA H^+ beam (10 keV) (a) and a 600 nA Ar_{40}^{17+} beam (95 MeV u^{-1}) (b) were used.

test of the HTS SQUID CCC which was installed in the beam transport line for the ECR (electron cyclotron resonance) ion source in the CNS experimental hall. After the measurement was successfully carried out in the CNS, we installed the system into the beam transport line (E1 experimental hall) of the RIKEN Ring Cyclotron (RRC) (figure 9) to measure the current of the high-energy heavy-ion beam which has a bunched microstructure. Figure 10 shows the measured signals of the HTS SQUID CCC (above) and those of the Faraday cup monitor (below) where a 7 μA H^+ beam (10 keV) (a) and a 600 nA Ar_{40}^{17+} beam (95 MeV u^{-1}) (b) were used.

5. Future research and development

Because the fluctuation of the measured ion beam current was 400 nA (standard deviation), an improvement of the detection resolution by more than two magnitudes is required. The possible reasons for the error due to noise are as follows: (1) as we did not use any batteries for the power supply of the SQUID circuit, the circuit might have been affected by AC power lines which contain noise, and (2) as the length between the control room and the experimental room where the THS SQUID CCC is installed is over 100 m, the signal cable might have been affected by the external RF noise of the ring cyclotron. Therefore, it is necessary to resolve these problems. From the viewpoint of the required efficiency of transferring the magnetic field produced by beams to a SQUID, the efficiency of the HTS SQUID CCC is inadequate. For example, the sensitivity of the HTS SQUID CCC is 30 pT/1 μA, while that of the LTS SQUID CCC, which was used in the heavy-ion cooler synchrotron TARN II, was 10 pT/1 nA [3]. The main reason for this difference is that it is too difficult to join the ends of a superconducting coil after it was wound around a high-permeability core. Consequently, the LTS SQUID CCC can make use of an input coil wound around the core, while the HTS-SQUID cannot use such an input coil; therefore, an input coil is built into the HTS SQUID itself. In order to improve the coupling efficiency between the SQUID sensor and the magnetic field generated by the beam, we are considering the possibility of introducing a high-permeability magnetic core into the HTS SQUID gradiometer (figure 11(a)). Figure 11(b) shows the magnetic field calculated using the

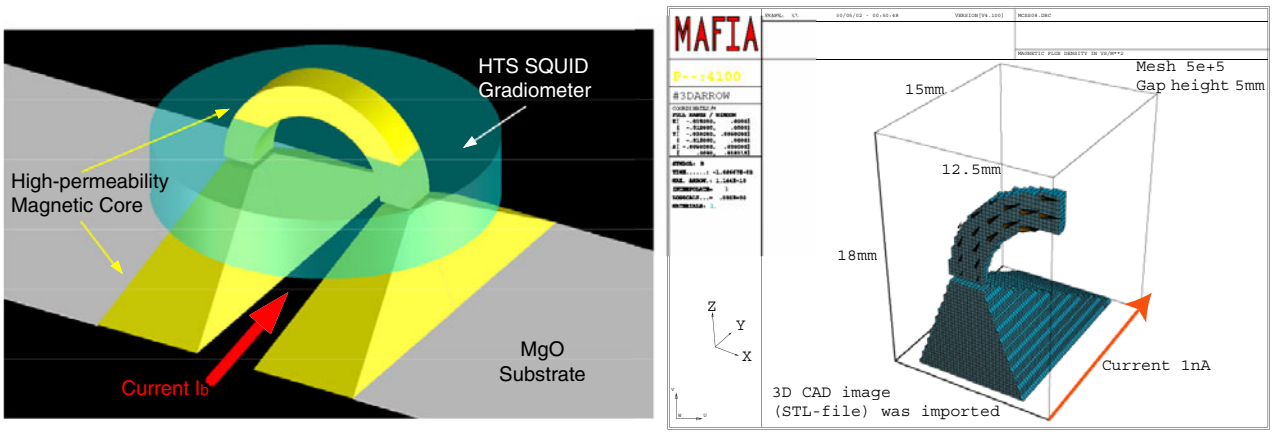

(a) (b)

Figure 11. (a) In order to improve the coupling efficiency between the SQUID sensor and the magnetic field generated by the beam, we are considering the possibility of introducing a high-permeability magnetic core into the HTS SQUID gradiometer. (b) The magnetic field calculated using the MAFIA program (see footnote 8) where 1 nA of current passes through the bridge.

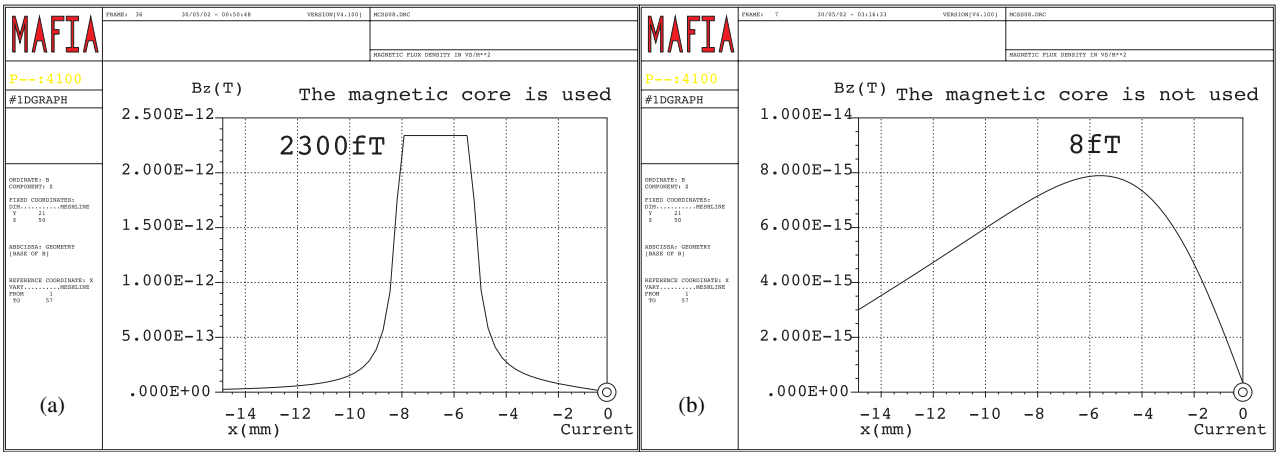

Figure 12. (a) The z-components of the calculated magnetic field B_z between two cores in accordance with the x axis are plotted. (b) The calculated magnetic field B_z when the high-permeability core is not used. This calculation shows that the signal was improved about 290 times when the high-permeability magnetic core was used.

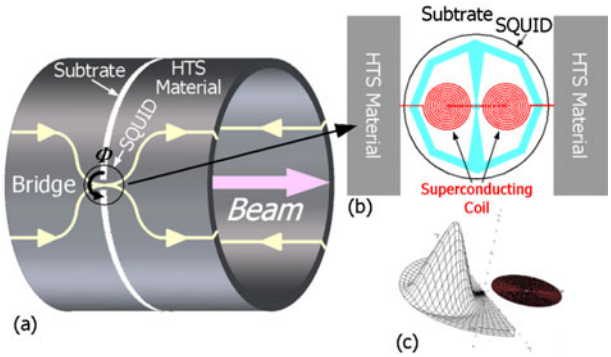

Figure 13. (a) A prototype current sensor with only a single-pass circuit at the bridge. (b) Stronger magnetic field is expected compared with the single pass circuit. (c) The shape of the magnetic field calculated by OPERA-3d. A 31-times stronger magnetic field was calculated compared with that in the case of a single-pass circuit when an 80 turn coil was used.

MAFIA program[8] where 1 nA of current passes through the bridge. MAFIA is an interactive program package for the computation of electromagnetic fields, and it is directly based on the fundamental equations of electromagnetic fields, the Maxwell equations. The z-components of the calculated magnetic field B_z between two cores in accordance with the x-axis are plotted in figure 12(a). Figure 12(b) represents the calculated magnetic field B_z when the high-permeability core is not used. This calculation shows that the signal was improved about 290 times, when the high-permeability magnetic core was used.

Furthermore, to increase the magnetic field induced at the bridge, we are researching the fabrication of a suitable superconducting coil. Figure 13(a) shows the prototype current sensor which has only a single-pass circuit at the bridge. However, if we can manufacture a superconducting coil and mount the SQUID at the bridge (figure 13(b)), a stronger magnetic field is expected compared with that in the case of the single-pass circuit. Figure 13(c) shows the shape of the magnetic field calculated by OPERA-3d. A 31-times stronger magnetic field is calculated compared with the single-pass circuit when an 80 turn coil is used. In addition, it was discovered that the beam position can be measured by dividing the current sensor into two parts and setting a SQUID on each bridge. Namely, it is possible to measure the beam current and beam position simultaneously in real time. We aim to measure the beam current and position of a 1 nA beam to make the system applicable to physics and biology experiments as well as to an ion implanter.

Acknowledgment

The authors are grateful to Robert L Fagaly of Tristan Technologies for valuable discussions on the HTS SQUID system.

References

[1] Unser K 1981 *IEEE Trans. Nucl. Sci.* **28** 2344
[2] Peters A *et al* 1998 *Proc. AIP Conf.* vol 451 (New York: American Institute of Physics) p 163
[3] Tanabe T *et al* 1999 *Nucl. Instrum. Methods Phys. Res.* A **427** 455
[4] Hao L *et al* 2001 *IEEE Trans. Appl. Supercond.* **11** 635
[5] Watanabe T *et al* 2002 *RIKEN Accel. Prog. Rep.* **35** 314
[6] Watanabe T *et al* 2002 *Proc. 8th Conf. on European Particle Accelerator 2002 (Paris, 3–7 June 2002)* (EPS-IGA) p 1995
[7] Watanabe T *et al* 2002 *CNS Annual Report* vol 59 (Tokyo, Japan: CNS, University of Tokyo) p 71
[8] Watanabe T *et al* 2003 *RIKEN Accel. Prog. Rep.* **36** 331
[9] Faley M I *et al* 2001 *IEEE Trans. Appl. Supercond.* **11** 1383
[10] Ishikawa Y *et al* 1992 *Adv. Supercond.* **4** 1073–6
[11] Watanabe S *et al* 2002 *Proc. 8th Conf. on European Particle Accelerator* p 1992

[8] AET Associates Inc., USA.